Supplementary Figures

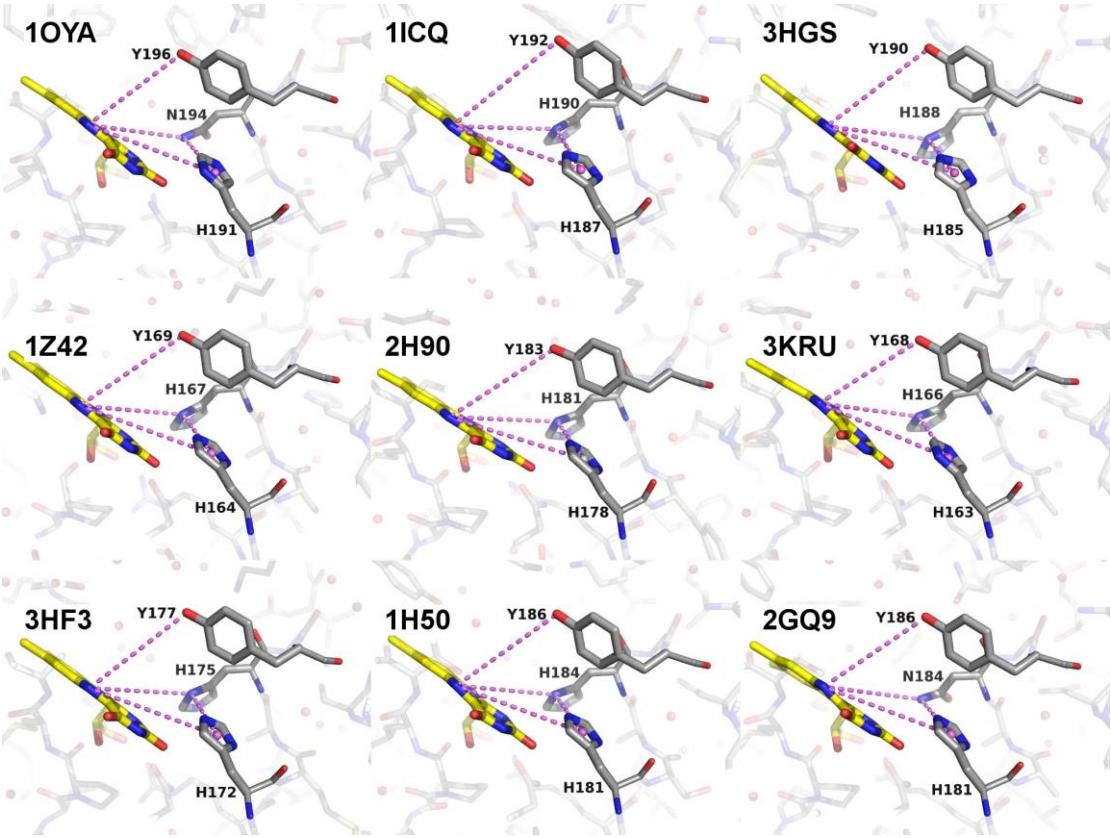

Supplementary Figure 1: OYE structures used to define the search template. **1OYA**: OYE from *Saccharomyces pastorianus*[1]; **1ICQ**: 12-oxophytodienoate reductase 1 from *Solanum lycopersicum*[2]; **3HGS**: 12-oxophytodienoate reductase 3 from *Solanum lycopersicum*[3]; **1Z42** YqjM from *Bacillus subtilis*[4]; **2H90**: xenobiotic reductase A from *Pseudomonas putida*[5]; **3KRU**: OYE from *Thermoanaerobacter pseudethanolicus* E39[6]; **3HF3**: OYE from *Thermus scotoductus* SA-01[7]; **1H50**: pentaerythritol tetranitrate reductase from *Enterobacter cloacae*[8]; **2GQ9**: SYE1 from *Shewanella oneidensis* MR-1[9]. Amino acid residues are shown in grey, the flavin cofactors in yellow. The distances d_1-d_4 are depicted as dashed magenta lines. The figure was prepared using the program PyMOL (Schrodinger Inc.).

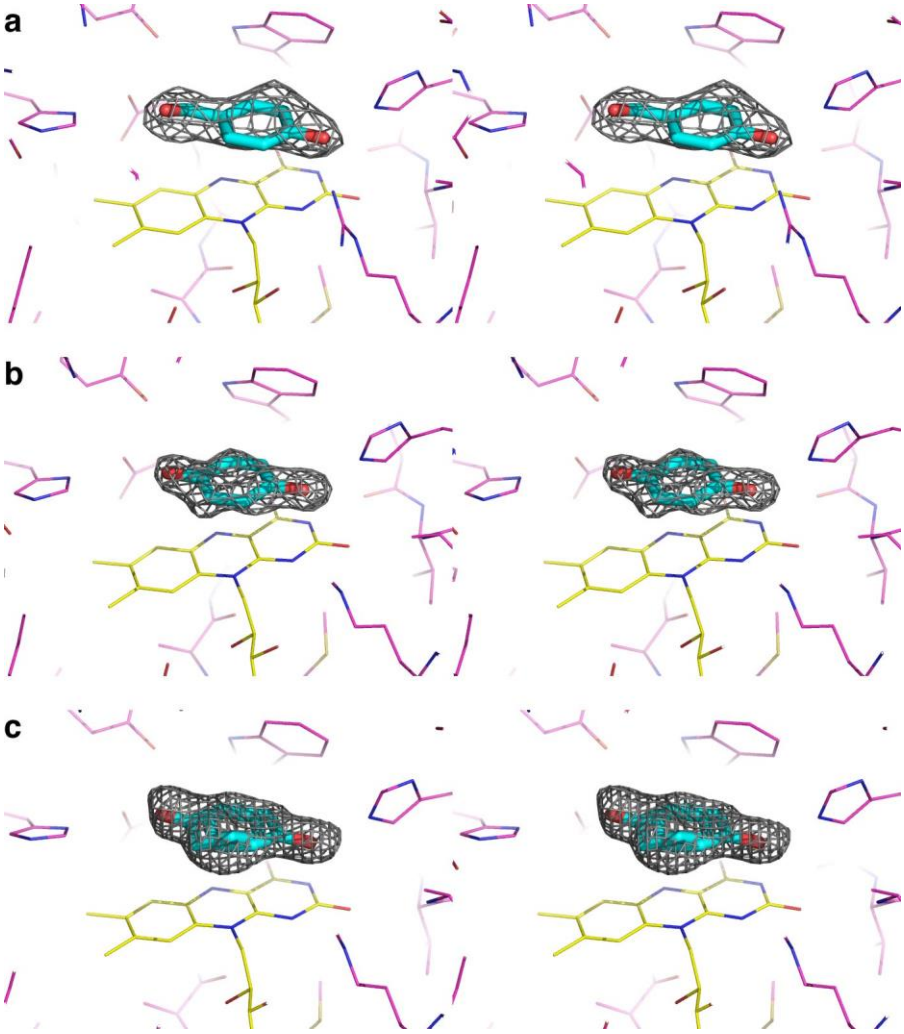

Supplementary Figure 2: Stereo representation of electron density maps of the bound ligands. *Fo-Fc* omit density (contoured at 3σ) of the complexes of *Ph*ENR with *p*-hydroxybenzaldehyde (**a**), 1,4-hydroquinone (**b**) and 2-cyclohexen-1-one (**c**). Amino acid residues are shown as purple lines, the flavin cofactors are shown in yellow. The bound ligands are shown as cyan sticks. The figure was prepared using the program PyMOL (Schrodinger Inc.).

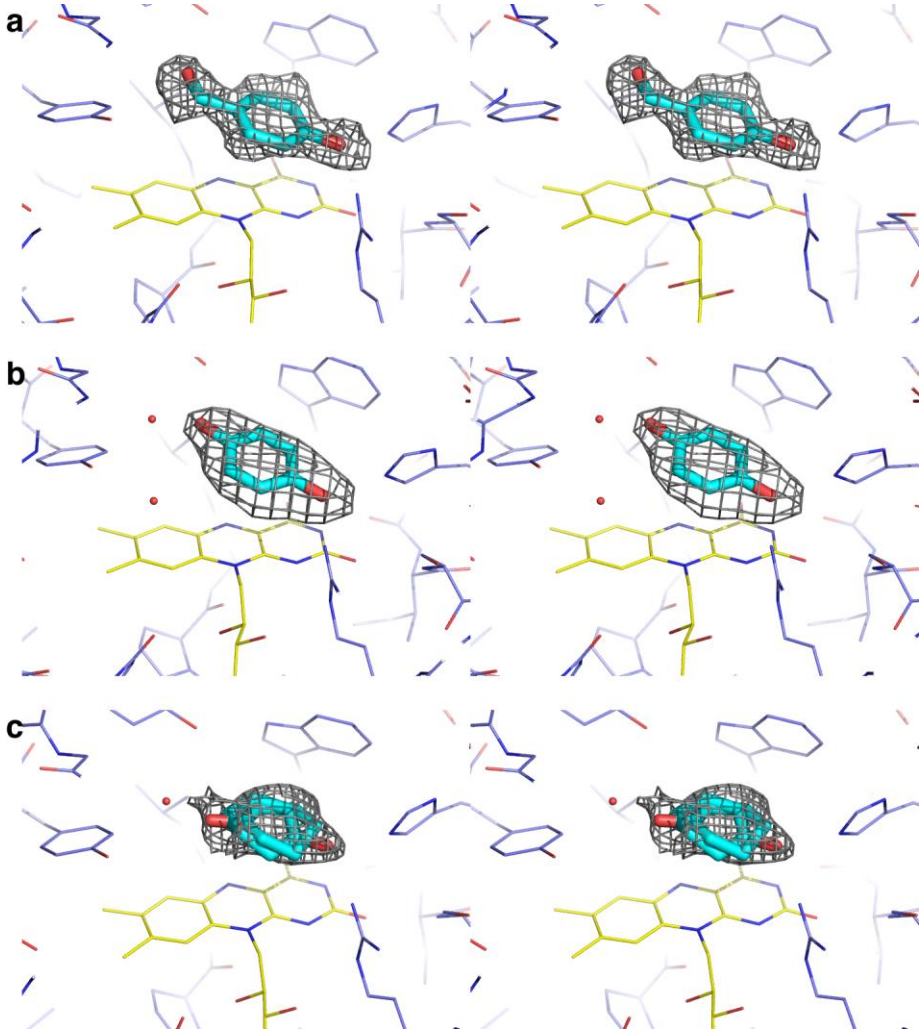

Supplementary Figure 3: Stereo representation of electron density maps of the bound ligands. *Fo-Fc* omit density (contoured at 3σ) of the complexes of *Tt*ENR with *p*-hydroxybenzaldehyde (**a**), 1,4-hydroquinone (**b**) and 2-cyclohexen-1-one (**c**). Amino acid residues are shown as dark blue lines, the flavin cofactors are shown in yellow. The bound ligands are shown as cyan sticks. The figure was prepared using the program PyMOL (Schrodinger Inc.).

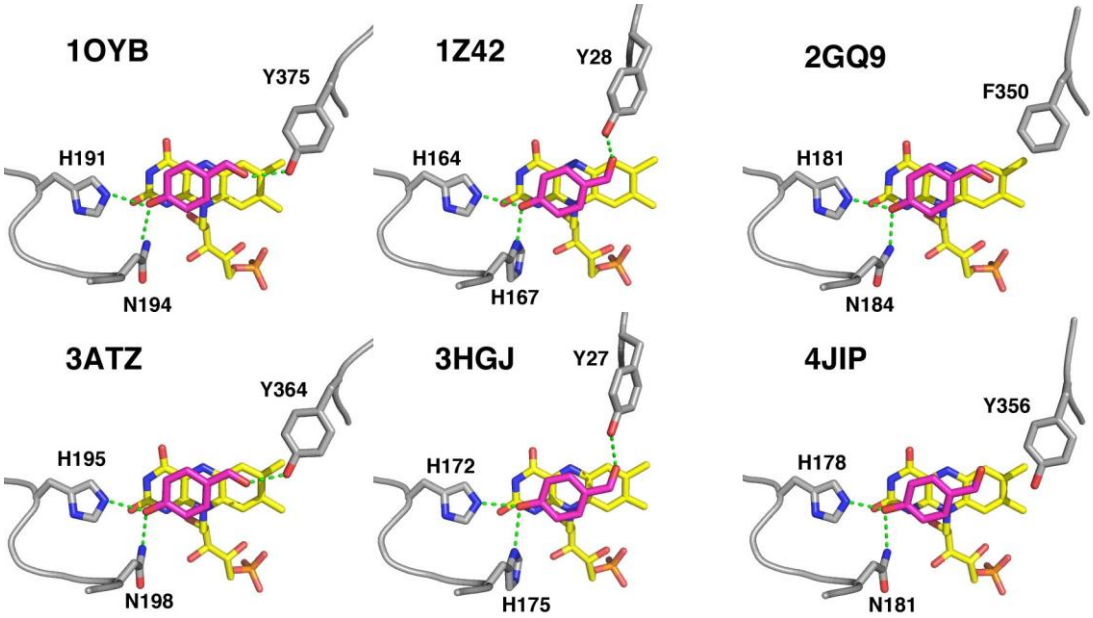

Supplementary Figure 4: Structures of OYEs in complex with *p*-hydroxybenzaldehyde, close-up view of the ligand binding site. **1OYB**: OYE from *Saccharomyces pastorianus*[1]; **1Z42** YqjM from *Bacillus subtilis*[4]; **2GQ9**: SYE1 from *Shewanella oneidensis* MR-1[9]; **3ATZ**: OYE from *Trypanosoma cruzi*[10]; **3HGJ**: OYE from *Thermus scotoductus*[7]; **4JIP**: glycerol trinitrate reductase NerA from *Agrobacterium radiobacter*[11]. Amino acid residues are shown in grey, the flavin cofactor in yellow and the bound ligand in magenta. Hydrogen bonds are depicted as green dashed lines. The figure was prepared using the program PyMOL (Schrodinger Inc.).

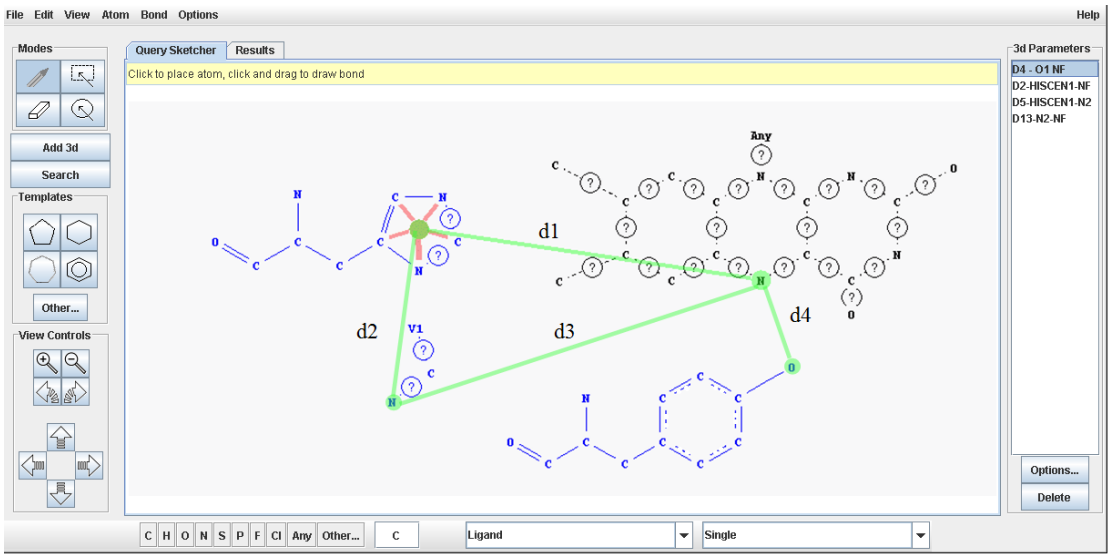

Supplementary Figure 5: Screenshot of the 2D/3D sketcher in Relibase+ with the definition of the search template. Since the sketcher does not show all defined 3D descriptors at once, the distance parameters (labeled d_1-d_4) were overlaid with green lines.

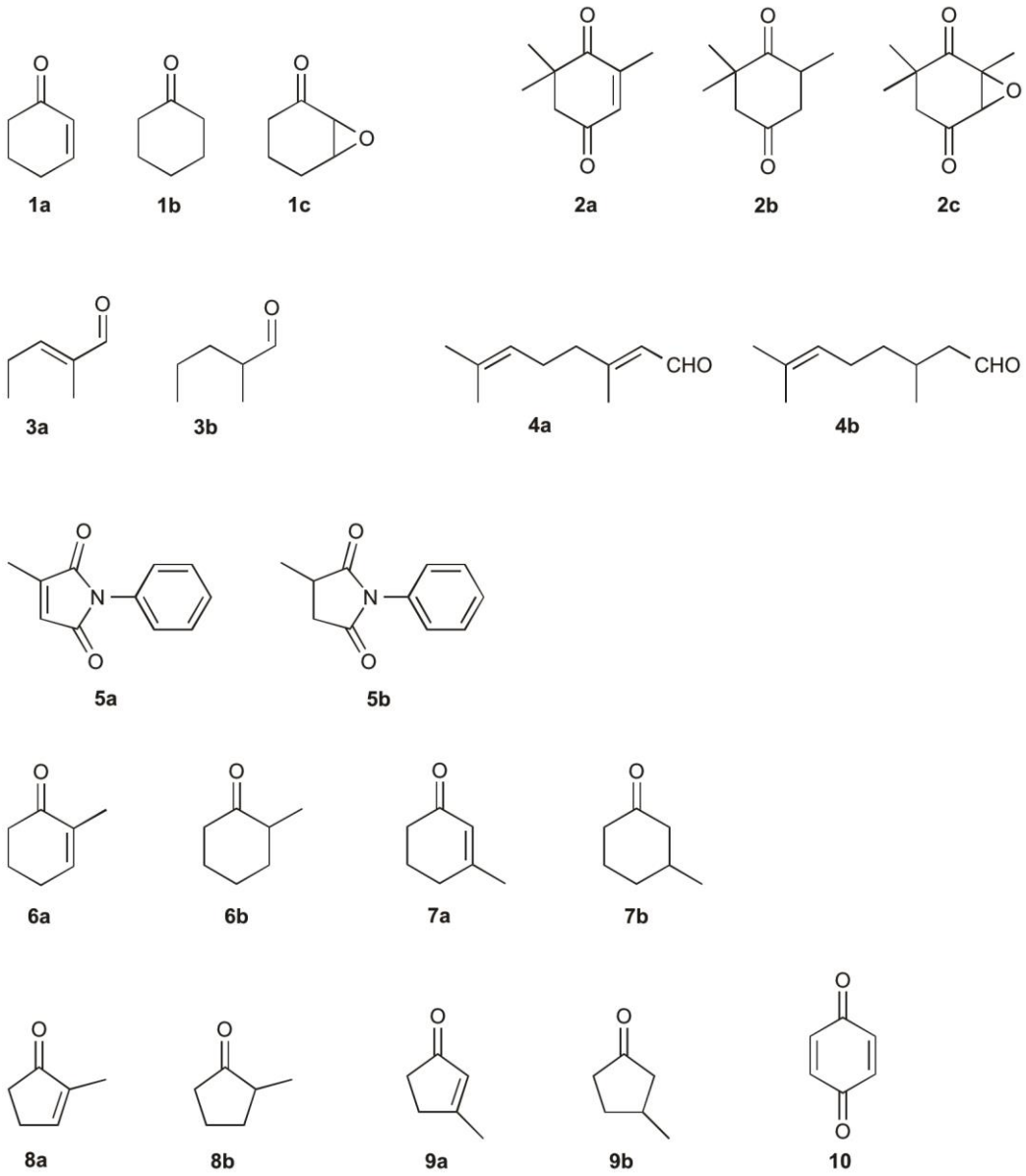

Supplementary Figure 6: Substrates (and reaction products) used for the biochemical characterization and the biocatalytic transformations.

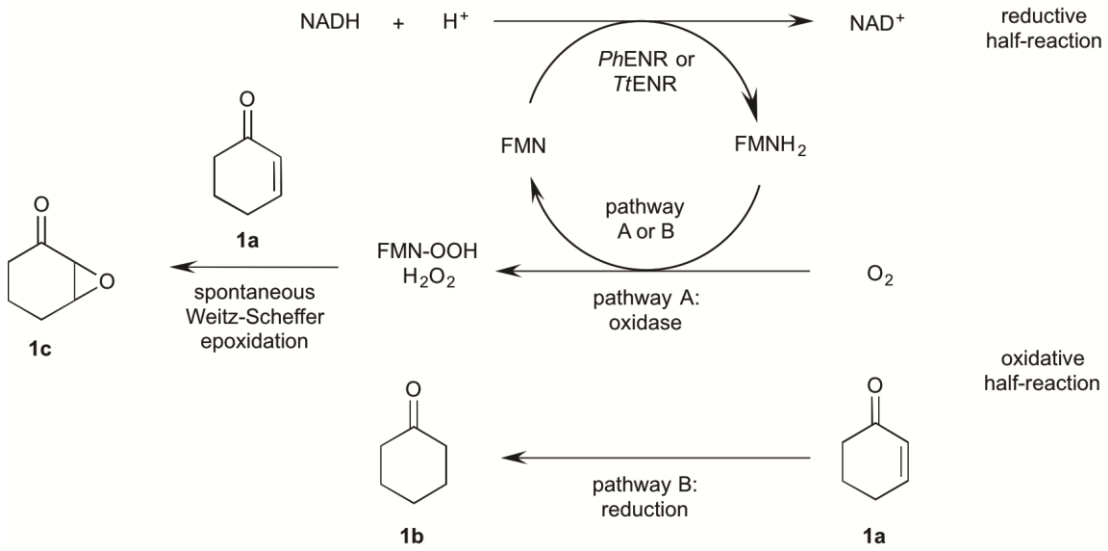

Supplementary Figure 7: Possible reaction pathways in the biocatalytic transformations. The reactive agent in the Weitz-Scheffer epoxidation is either the flavin-hydroperoxide intermediate or hydrogen peroxide produced by the oxidation of reduced FMN by molecular oxygen.

Supplementary Tables

Supplementary Table 1: Distances between crucial active site residues in structures of Old Yellow Enzymes.

PDB-entry	distances [Å]			
	d_1[a,e]	d_2[b,e]	d_3[c]	d_4[d]
1OYA	7.6	4.7	6.1	6.6
1ICQ	7.6	4.9	6.5	7.7
3HGS	7.6	4.7	6.5	7.2
1Z42	7.8	4.6	6.5	6.9
2H90	7.9	4.7	6.7	7.0
3KRU	7.7	4.8	6.4	6.6
3HF3	7.6	4.7	6.4	6.9
1H50	7.6	4.8	6.3	7.0
2GQ9	7.6	4.8	6.4	6.9

[a]pseudoatom center of His to FMN-N5

[b]pseudoatom center of His to His-ND1 or Asn-ND2

[c]His-ND1 or Asn-ND2 to FMN-N5

[d]Tyr-OH to FMN-N5

[e]pseudoatoms were placed at the geometric centers of the imidazole rings

Supplementary Table 2: Result of the catalophore search.

protein	PDB-entry	
FMN-binding protein from *Pyrococcus horikoshii*	**2R6V**	non-OYE hits
putative styrene monooxygenase small component from *Thermus thermophilus*	**1USC, 1USF**	non-OYE hits
cholesterol oxidase from *Brevibacterium sterolicum*	2I0K	non-OYE hits
oxidoreductase from *Agrobacterium fabrum*	3FBS	non-OYE hits
flavocytochrome C from *Shewanella frigidimarina*	1JRZ	non-OYE hits
OYE from *Saccharomyces pastorianus*	**1OYA***, 1OYB, 1OYC, 1K02	hits of known OYE structures including structures used for template generation(*)
OPR-1 from *Solanum lycopersicum* and from *Arabidopsis thaliana*	**1ICQ***, 1ICP, 1ICS, 3HGR, 2Q3O, 2Q3R	hits of known OYE structures including structures used for template generation(*)
OPR-3 from *Solanum lycopersicum* and from *Arabidopsis thaliana*	**3HGS***, 3HGO, 2Q3O	hits of known OYE structures including structures used for template generation(*)
YqjM from *Bacillus subtilis*	**1Z42***, 1Z41, 1Z44, 1Z48	hits of known OYE structures including structures used for template generation(*)
xenobiotic reductase A from *Pseudomonas putida*	**2H90***, 2H8Z, 2H8X	hits of known OYE structures including structures used for template generation(*)
thermostable OYE from *Thermoanaerobacter pseudethanolicus*	**3KRU***, 3KRZ	hits of known OYE structures including structures used for template generation(*)
OYE from *Thermus scotoductus*	**3HF3***, 3HGJ	hits of known OYE structures including structures used for template generation(*)
pentaerythritol tetranitrate (PETN) reductase from *Enterobacter cloacae*	**1H50***, 1H51, 1H60, 1H61, 1H62, 1H63, 3F03, 2ABA, 1VYR, 1GVR, 1GVS, 1GVO, 1GVQ, 2ABB, 1VYP, 3KFT	hits of known OYE structures including structures used for template generation(*)
SYE-1 from *Shewanella oneidensis*	**2GQ9***, 2GQ8, 2GQA	hits of known OYE structures including structures used for template generation(*)
N-ethylmaleimide reductase from *Burkholderia pseudomallei*	3GKA	hits of known OYE structures including structures used for template generation(*)

Supplementary Table 3: Data collection and refinement statistics.

	***Ph*ENR, 2-cyclo-hexen-1-one**	***Ph*ENR, *p*HB**	***Ph*ENR, 1,4-hydro-quinone**	***Tt*ENR, 2-cyclo-hexen-1-one**	***Tt*ENR, *p*HB**	***Tt*ENR, 1,4-hydro-quinone**
Data collection						
Space group	$P6_122$	$P6_122$	$P6_122$	$P2_1$	$P2_12_12_1$	$P2_12_12_1$
Cell dimensions						
a, *b*, *c* (Å)	46.1, 46.1, 269.0	46.3, 46.3, 268.9	46.4, 46.4, 269.6	63.8, 73.8, 77.4	64.7, 74.9, 77.6	64.5, 74.6, 77.7
α, β, γ (°)	90, 90, 120	90, 90, 120	90, 90, 120	90, 90.1, 90	90, 90, 90	90, 90, 90
Resolution (Å)	45-1.75 (1.85-1.75)*	20-2.10 (2.20-2.10)*	40-1.68 (1.78-1.68)*	30-1.65 (1.75-1.65)*	38-1.70 (1.80-1.70)*	50-2.15 (2.28-2.15)*
R_{meas}	0.058 (0.675)	0.060 (0.291)	0.068 (0.501)	0.060 (0.720)	0.082 (0.525)	0.105 (0.626)
$I / \sigma I$	26.2 (3.5)	21.4 (4.3)	22.6 (3.7)	16.5 (2.3)	16.0 (3.3)	12.7 (3.4)
Completeness (%)	100 (100)	85.1 (90.0)	89.2 (91.6)	99.4 (97.0)	92.7 (96.0)	99.0 (96.8)
Redundancy	15.3 (10.8)	7.8 (3.8)	11.2 (9.5)	4.2 (3.8)	5.9 (6.2)	9.3 (8.3)
Refinement						
Resolution (Å)	45-1.75	20-2.10	40-1.68	30-1.65	38-1.70	50-2.15
No. reflections	18259 (2711)	9300 (1218)	18582 (3000)	86300 (13487)	39042 (6287)	20947 (3245)
R_{work} / R_{free}	0.194 / 0.230	0.242 / 0.269	0.213 / 0.249	0.161 / 0.186	0.242 / 0.277	0.192 / 0.249
No. atoms						
Protein	1476	1408	1488	5828	2786	2811
Ligand/cofactor	45	40	39	180	80	78
Water	62	18	93	620	173	111
B-factors (Å^2)						
Protein	30.8	25.8	23.5	22.2	19.1	49.1
Ligand/cofactor	18.9	17.6	15.1	21.8	17.8	40.6
Water	38.5	30.7	34.4	32.7	20.4	50.3
R.m.s. deviations						
Bond lengths (Å)	0.008	0.012	0.012	0.006	0.015	0.010
Bond angles (°)	1.3	1.7	1.6	1.2	1.8	1.5
PDB-entry	3ZOG	3ZOC	3ZOD	3ZOH	3ZOE	3ZOF

*Highest resolution shell is shown in parentheses.

Supplementary Table 4: Biocatalytic transformations of typical Old-Yellow-Enzymes.

Substrate	OPR1[12,13]		OPR3[12,13]		YqjM[13]		OYE1[14]	
	c [%]	*e.e.* [%]	*c* [%]	*e.e.* [%]	*c* [%]	*e.e.* [%]	*c* [%]	*e.e.* [%]
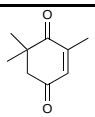 **2a**	95-98	51-91 (*R*)	95-98	33-99 (*R*)	86-96	37-99 (*R*)	88-99	39-98 (*R*)
 **3a**	96	47 (*R*)	70	19 (*S*)	78	10 (*R*)	-	-
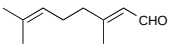 **4a**	15-99	>95 (*S*)	90-95	>95 (*S*)	57-70	>95 (*S*)	49-98	15 (*S*) – 77 (*R*)
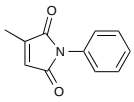 **5a**	99	96-99 (*R*)	99	92-99 (*R*)	98-99	92-99 (*R*)	>99	72-75 (*R*)

c: conversion, *e.e.*: enantiomeric excess,
OPR1: 12-oxophytodienoate reductase isoform 1 from *Lycopersicon esculentum* (tomato),
OPR3: 12-oxophytodienoate reductase isoform 3 from *Lycopersicon esculentum* (tomato),
YqjM: Old-Yellow-Enzyme homolog from *Bacillus subtilis*,
OYE1: Old-Yellow-Enzyme from *Saccharomyces cerevisiae*

Supplementary Table 5: Optimization of reaction conditions.

				*Tt*ENR		*Ph*ENR	
	conditions[a]	*T* [°C]	*pH*	NADH	NADPH	NADH	NADPH
				c [%]	*c* [%]	*c* [%]	*c* [%]
1	buffer A, aerobic	30	7	19	**20**	20	**>99**
2			8	9	15	15	67
3			9	4	8	8	<1
4	buffer A, anaerobic	30	7		19		**>99**
5			8		7		80
6	buffer B, anaerobic		6.2		17		98
7			7		**27**		80
8			7.5		21		
9			8		12		
10[b]	buffer B, anaerobic	30	7		**15**		
11[b]		40			14		
12[b]		50			12		
13[b]	buffer A, anaerobic	30	7				**40**
14[b]		40					37
15[b]		50					36

[a]buffer A: 50 mM Tris/HCl buffer; buffer B: 50 mM phosphate buffer; [b]in an Eppendorf thermomixer at 300 rpm;

Supplementary Methods

GC- and HPLC-analytics

GC–FID analyses were carried out with a Varian 3800 GC-FID chromatograph (Palo Alto, CA, USA) using a J&W HP-5 5% phenylmethylpolysiloxane capillary column (30 m x 0.32 mm, 0.25 µm film, Agilent, St. Clara, CA, USA) using H_2 as a carrier gas (14.5 psi). HPLC analyses were performed using a Shimadzu LC-20AD system (Kyoto, Japan) equipped with a with a SPD-M20A diode array detector.

For achiral GC, the injector and detector temperatures were set to 300 °C, the split ratio was 20:1. Temperature program for **1-4** and **6-9** was: 40 °C hold 2 min, 20 °C min^{-1} to 180 °C, hold 8 min. Retention times were as follows: **1a**: 5.9 min, **1b**: 5.5 min, **1c**: 7.0 min, **2a**: 8.1 min, **2b**: 8.3 min, **2c**: 7.9 min, **3a**: 4.7 min, **3b**: 3.9 min, (*Z*)-**4a**: 9.0 min, (*E*)-**4a**: 9.3 min, **4b**: 8.2 min, **6a**: 6.1 min, **6b**: 5.1 min, **7a**: 7.3 min, **7b**: 6.2 min, **8a**: 5.6 min, **8b**: 4.8 min, **9a**: 6.3 min, **9b**: 4.9 min. Temperature program for **5**: 100 °C hold 0.5 min, 10 °C min^{-1} to 280 °C, hold 2 min. Retention times were as follows: **5a**: 10.3 min, **5b**: 11.1 min.

The enantioselectivity for **2b**, **3b**, **4b** and **12b** was determined by chiral GC-FID. For **2b** and **3b** a Varian Chirasil-Dex CB capillary column (25 m x 0.32 mm, 0.25 µm film, Palo Alto, CA, USA), injector and detector temperatures of 200 °C and a 20:1 split ratio were used. The temperature program for **2b** was: 90 °C hold 2 min, 4 °C min^{-1} to 115 °C, 20 °C min^{-1} to 180 °C hold 2 min. Retention times were: (*R*)-**2b**: 10.99 min, (*S*)-**2b**: 11.05 min. **3b** was analyzed as the corresponding alcohol (2-methylpentanol). For the reduction of **3b** $CeCl_3$ (37 µL, 10 % $CeCl_3$ x 7 H_2O in water) was added. After mixing and addition of $NaBH_4$ (37 µl, 1% $NaBH_4$ in H_2O) the vial was shaken for 1 h at 40 °C and the workup was continued as described above. The temperature program was: 40 °C hold 0 min, 10 °C min^{-1} to 60 °C hold 6 min, 10 °C min^{-1} to 180 °C. Retention times were 11.9 min (*R*) and 12.0 min (*S*). For **4b** a Hydrodex-β-TBDAc capillary column, 25 m x 0.25 mm, injector and detector temperatures of 250 °C and a 20:1 split ratio were used. The temperature program for **4b** was 80 °C hold 2 min, 1 °C min^{-1} to 95 °C, 0.5 °C min^{-1} to 100 °C hold 5 min, 10 °C min^{-1} to 180 °C. Retention times were: (*S*)-**4b**: 29.5 min, (*R*)-**4b**: 30.1 min. For **8b** a Supelco Chiraldex B-TA capillary column (40 m x 0.32 mm x 0.12 µm film, Sigma Aldrich, St. Louis, MO,

USA), injector and detector temperatures of 200 °C and a 20:1 split ratio were used. The temperature program for **8b** was 70 °C hold 8 min, 10 °C min^{-1} to 80 °C hold 2 min, 30 °C min^{-1} to 180 °C. Retention times were: (*R*)-**8b**: 11.54 min, (*S*)-**8b**: 11.68 min. The enantioselectivity for **5b** was determined by HPLC using a Chiralcel OD-H column (25 cm x 0.46 cm, Chiral Technologies, Illkirch, France) and *n*-heptane/EtOH, 95:5 (isocratic) at 18 °C. Retention times were: (*R*)-**5b**: 33.9 min, (*S*)-**5b**: 38.4 min.

The absolute configurations of **2b**, **3b**, **5b** and **8b** were determined by co-injection with reference materials of known absolute configuration[13] as follows: **2b**: bioreduction with bakers yeast produced (*R*)-**2b** with 62% e.e.; **3b**: bioreduction with OPR1 produced (*R*)-**3b** with 47% e.e.; **5b**: bioreduction with OYE1 produced (*R*)-**5b** with 99% e.e.; **8b**: bioreduction with OPR1 produced (*S*)-**8b** with 61% e.e. The absolute configuration of **4b** was determined by co-injection with commercially available (*S*)-citronellal (*S*)-**4b** (Sigma Aldrich, St. Louis, MO, USA).

Supplementary References

1 Fox, K. M. & Karplus, P. A. Old yellow enzyme at 2 Å resolution: Overall structure, ligand binding, and comparison with related flavoproteins. *Structure* **2**, 1089-1105 (1994).

2 Breithaupt, C. *et al.* X-ray structure of 12-oxophytodienoate reductase 1 provides structural insight into substrate binding and specificity within the family of OYE. *Structure* **9**, 419-429 (2001).

3 Breithaupt, C. *et al.* Structural basis of substrate specificity of plant 12-oxophytodienoate reductases. *J. Mol. Biol.* **392**, 1266-1277 (2009).

4 Kitzing, K. *et al.* The 1.3 Å crystal structure of the flavoprotein YqjM reveals a novel class of Old Yellow Enzymes. *J. Biol. Chem.* **280**, 27904-27913 (2005).

5 Griese, J. J., P. Jakob, R., Schwarzinger, S. & Dobbek, H. Xenobiotic reductase A in the degradation of quinoline by *Pseudomonas putida* 86: Physiological function, structure and mechanism of 8-hydroxycoumarin reduction. *J. Mol. Biol.* **361**, 140-152 (2006).

6 Adalbjörnsson, B. V. *et al.* Biocatalysis with thermostable enzymes: Structure and properties of a thermophilic 'ene'-reductase related to old yellow enzyme. *ChemBioChem* **11**, 197-207 (2010).

7 Opperman, D. J. *et al.* Crystal structure of a thermostable old yellow enzyme from *Thermus scotoductus* SA-01. *Biochem. Biophys. Res. Co.* **393**, 426-431 (2010).

8 Barna, T. M. *et al.* Crystal structure of pentaerythritol tetranitrate reductase: "Flipped" binding geometries for steroid substrates in different redox states of the enzyme. *J. Mol. Biol.* **310**, 433-447 (2001).

9 van den Hemel, D., Brige, A., Savvides, S. N. & Van Beeumen, J. Ligand-induced conformational changes in the capping subdomain of a bacterial Old Yellow Enzyme homologue and conserved sequence fingerprints provide new insights into substrate binding. *J. Biol. Chem.* **281**, 28152-28161 (2006).

10 Okamoto, N. *et al.* Structural insight into the stereoselective production of PGF2α by Old Yellow Enzyme from *Trypanosoma cruzi*. *J. Biochem.* **150**, 563-568 (2011).

11 Oberdorfer, G. *et al.* The structure of glycerol trinitrate reductase NerA from *Agrobacterium radiobacter* reveals the molecular reason for nitro- and ene-reductase activity in OYE homologues. *ChemBioChem* **14**, 836-845 (2013).

12 Hall, M., Stueckler, C., Kroutil, W., Macheroux, P. & Faber, K. Asymmetric bioreduction of activated alkenes using cloned 12-oxophytodienoate reductase isoenzymes OPR-1 and OPR-3 from *Lycopersicon esculentum* (tomato): A striking change of stereoselectivity. *Angew. Chem. Int. Ed.* **46**, 3934-3937 (2007).

13 Hall, M. *et al.* Asymmetric bioreduction of C=C bonds using enoate reductases OPR1, OPR3 and YqjM: Enzyme-based stereocontrol. *Adv. Synth. Catal.* **350**, 411-418 (2008).

14 Hall, M. *et al.* Asymmetric bioreduction of activated C=C bonds using *Zymomonas mobilis* NCR enoate reductase and old yellow enzymes OYE 1-3 from yeasts. *Eur. J. Org. Chem.*, 1511-1516 (2008).